Seitz, F.; Stuck, J.; Thomas, M.: White noise Chandler wobble excitation.

In: Plag, H.-P.; Chao, B.; Gross, R.; van Dam, T. (eds.) Forcing of polar motion in the Chandler frequency band: A contribution to understanding interannual climate variations, Cahiers du Centre Européen de Géodynamique et de Séismologie, Vol. 24, pp 15-21, European Center for Geodynamics and Seismology (ECGS) , ISBN (Print) 2-9599804-1-7, 2005.

In: Forcing of Polar Motion in the Chandler Frequency Band: A Contribution to Understanding Interannual Climate Variations, H.-P. Plag et al (Eds.), Cahiers du Centre Européen de Géodynamique et de Séismologie, Vol. 24, 15-21, Luxembourg

White noise Chandler wobble excitation

Florian Seitz
Deutsches Geodätisches Forschungsinstitut (DGFI), Marstallplatz 8, D-80539 Munich, Germany
e-mail: florian.seitz@dgfi.badw.de

Jochen Stuck
GeoForschungsZentrum Potsdam (GFZ), Telegrafenberg, D-14473 Potsdam, Germany

Maik Thomas
Institut für Planetare Geodäsie (IPG), TU Dresden, Mommsenstrasse 13, D-01062 Dresden, Germany

Abstract. In order to increase the understanding of both geophysically induced global mass transports and the dynamical response of the Earth, the non-linear dynamic Earth system model DyMEG has been developed at Deutsches Geodätisches Forschungsinstitut (DGFI). The model is forced by time series of consistent atmospheric and oceanic angular momentum variations. Besides, gravitational effects and deformations due to loading and rotational variations are regarded. The numerical results for polar motion from DyMEG are significantly related with geodetic observations. Depending on the quality of the excitations, the correlation coefficients between the unconstrained model time series and the observations amount to 0.99. Analyses of the polar motion series show, that the simulated Chandler wobble from DyMEG is excited by atmospheric and oceanic mass redistributions over more than two decades. This study demonstrates that the damping of the Chandler amplitude is counteracted by noise, which is contained in the atmospheric and oceanic excitation series due to stochastic weather processes. Numerical experiments with synthetic white noise excitation show, that the noise level which is necessary to perpetuate the Chandler amplitude is just as high as the noise level which is provided by the atmospheric and oceanic forcing fields.

1 Introduction

Since a few decades, space geodetic techniques provide time-series of Earth orientation parameters with increasing accuracy. The fluctuations of Earth rotation, reflected by polar motion and changes in length-of-day, are integral quantities which are associated with the mass redistributions and motions occurring in the Earth's subsystems. Usually, it is very difficult to associate a particular variation with a given cause. On seasonal time scales, the largest effects are due to tidal deformations of the solid Earth and mass redistributions within the atmosphere and the oceans. Variations of Earth rotation caused by these excitations are additionally superposed by free oscillations of the Earth, i.e., the Chandler wobble and the nearly diurnal free wobble. It is well known that the amplitude of the Chandler wobble would diminish due to friction without further excitation (Munk and MacDonald, 1960). However, spectral analyses of geodetic observations reveal significant amplitude variations of the Chandler oscillation which implies the existence of some excitation mechanism. The reason for the perpetuation of the Chandler amplitude is still under investigation. By now, it seems to be understood that the Chandler wobble is excited by a combined effect of atmosphere and ocean. However the individual contributions of these two subsystems could not be fully assessed.

The Chandler wobble is a resonance oscillation of the Earth. To excite the Earth's free polar motion and thus to counteract its damping, potential excitation mechanisms require energy in a band close to the Chandler frequency. But spectral analyses give no hint for increased excitation energy in either spectra of atmospheric and oceanic excitations in the Chandler band (Gross, 2000; Stuck et al., 2005). Though different patterns of climate variability exist on interannual time scales (e.g. the Quasi-Biennial Oscillation, the North Atlantic Oscillation or El Niño), none of these phenomena gives rise to any periodic or quasi-periodic excitation mechanism in the

Chandler frequency range as they affect differing parts of the spectrum. However, ongoing stochastic weather phenomena yield a random distribution of excitation energy in the atmospheric and oceanic time series over the whole spectrum (white noise). The present paper enters into the question if the excitation energy of this flat distribution provides sufficient energy to provoke a resonant reaction of the rotating Earth via rotational deformations.

2 Dynamic Earth system model DyMEG

The dynamic Earth system model DyMEG (Dynamic Model for Earth Rotation and Gravity) has been developed in order to study the Earth's reaction on gravitational and geophysical excitations (Seitz and Kutterer, 2002). It is based on the balance of angular momentum in the Earth system, which is described by the non-linear Liouville differential equation in a rotating reference frame (Munk and MacDonald, 1960). The model is forced by consistent time series of variations of the Earth's tensor of inertia and relative angular momenta which are deduced from consistent atmospheric and oceanic reanalyses or circulation models. The indirect effect due to load deformations is computed via Green's functions.

In contrast to former investigations, the characteristics of the Earth's free polar motion (Chandler wobble) are not explicitly predetermined with respect to period and damping but reproduced by the model from geometrical and rheological parameters. Therefore the traditional analytical solution is not applicable, and the Liouville equation is solved numerically as an initial value problem. A sensitivity analysis of DyMEG revealed, that the solution based on a Runge-Kutta method is reliable from an algorithmic point of view, and that the dependence with respect to the initial values, which are deduced from the observation time series C04 of the IERS is uncritical (Seitz and Kutterer, 2002). Traditionally, the Liouville equation is solved analytically which requires its linearisation. Due to the numerical approach, linearisation is not necessary in DyMEG. The Earth ellipsoid on which the model is based, is approximated by a triaxial tensor of inertia. It is characterised by different equatorial principal moments of inertia A and B.

The period of the Earth's free wobble is lengthened from the Euler period of 304 days (which would be the period if the Earth was rigid) to the observed Chandler period of about 434 days due to rotational deformations (Smith and Dahlen, 1981). This back-coupling mechanism of rotational variations causes perturbations of the second-degree spherical harmonic geopotential coefficients ΔC_{21} and ΔS_{21}. The coefficients are directly linked to the elements $\Delta\underline{\mathbf{I}}_{13}$ and $\Delta\underline{\mathbf{I}}_{23}$ of the symmetric tensor of inertia, which have the largest influence on polar motion (Munk and MacDonald, 1960). Hence time-varying mass distributions are accompanied by modified resonance conditions and thus affect the free polar motion of the model.

Within a sensitivity analysis of DyMEG, the dependence of the numerical solution was assessed with respect to model parameters which are entered into the model. In particular, the effect of the complex pole tide Love number k_2 was discussed, which is a critical parameter when the effects of rotational deformations are computed (Munk and MacDonald, 1960). The numerical value of k_2 is directly linked to period and damping of the simulated Chandler wobble from DyMEG. For $k_2 = 0.3520 + 0.0042\,i$ (corresponding to a period of 434 days and a quality factor of $Q = 68$), the resulting model time series show optimum agreement with geodetic observations. This value, which was determined empirically (Seitz and Kutterer, 2005), comprehends the effects of ocean pole tides and the anelastic response of the Earth's mantle.

3 Consistent atmospheric and oceanic excitation of polar motion

For atmospheric and oceanic forcing, two independent consistent model combinations are considered. First, atmospheric data based on the reanalyses of the National Centers of Environmental Prediction (NCEP) (Kalnay et al., 1996) were applied in combination with the ocean model ECCO (Stammer et al., 2003). The combination NCEP-ECCO is a consistent representation of dynamics and mass motions in the subsystems atmosphere and ocean because NCEP forcing fields are used for the computation of ocean dynamics in ECCO. As atmospheric pressure forcing is excluded, the ocean's response to pressure variations is assumed to be exact inverse barometric. The simulations cover a range of 23 years from 1980 until 2002. Second, the atmospheric model ECHAM3-T21

GCM (DKRZ, 1992), which is driven by observed sea surface temperature (SST) fields and global ice coverage, was used in combination with the ocean model OMCT for circulation and tides (Thomas et al., 2001) which is driven by ECHAM3. Both models and their coupling are described in detail by Seitz et al. (2004). As atmospheric pressure forcing is taken into account by OMCT (and consequently the pressure driven circulation), the two considered model combinations differ with respect to the pressure coupling. The ECHAM3-OMCT simulation covers a range of 20 years from 1975 until 1994. As the NCEP data set is based on atmospheric observations, the combination NCEP-ECCO is expected to correspond better with reality than ECHAM3-OMCT. The latter models are completely free. Apart from the SST-boundary conditions, the dynamics of the atmosphere and the oceans are solely based on model physics.

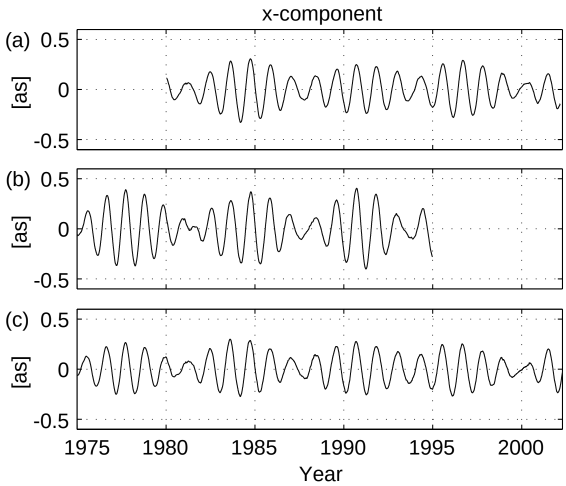

Figure 1. Model results for polar motion (x-component) applying combined atmospheric and oceanic excitations. (a) NCEP - ECCO, (b) ECHAM3 - OMCT, (c) geodetic observation C04. Linear trends have been removed.

3.1 Combined atmospheric and oceanic forcing

The model time series for the x-component of polar motion resulting from atmospheric and oceanic forcing are displayed in Fig. 1. Due to the nearly circular trait of Chandler and annual wobble, the y-components look similar. For NCEP-ECCO (top), the correlation coefficients with the geodetic observations (bottom) are 0.98 for the x- and 0.99 for the y-component (not shown). The respective RMS-values are 29.5 mas and 23.3 mas. Both annual and Chandler amplitude (x-component: 85 and 186 mas; y-component: 79 and 186 mas) are in good agreement with the observations (x-component: 82 and 180 mas; y-component: 76 and 180 mas). In the case of ECHAM3-OMCT (middle) the correlation coefficients amount to 0.95 and 0.94 for x- and y-component respectively, the corresponding RMS-values are 70.8 mas and 75.8 mas. Here, the agreement is slightly lower as the annual signal is overestimated by ECHAM3. In both components, the annual amplitude is 168 mas and the Chandler amplitude amounts to 202 mas.

Both model combinations lead to an undamped polar motion of DyMEG. Signal analyses of the resulting time series by means of wavelet transformation feature stable energy in the Chandler frequency band. Hence, the consistent atmospheric and oceanic forcing is capable of exciting the Chandler amplitude over more than two decades. In the following, the effects of atmospheric and oceanic excitations are studied separately in order to discover the prominent hurrier of the free polar motion.

3.2 Separated atmospheric and oceanic forcing

The computations of polar motion with separated atmospheric and oceanic forcing span the epoch between 1.1.1980 and 31.12.1994 which is covered by all four excitation series. This is done in order to avoid discrepancies between the results which are due to differing initial conditions and thus might lead to misinterpretations. In Fig. 2, the time series resulting from atmospheric (NCEP, ECHAM3) and oceanic (ECCO, OMCT) forcing are displayed (x-components). Both atmospheric and oceanic excitations contribute significantly to polar motion. However, the time series feature noticeable discrepancies among each other. Most obviously, the results differ with respect to the amplitudes of Chandler and annual signals. Besides, the period of the free wobble which was determined by a Fourier analysis of the model time series is slightly shifted: With atmospheric excitations, the resulting Chandler period is 432 days (NCEP) and 431 days (ECHAM3) respectively; using oceanic forcing, the period is unchanged with ECCO (434 days) but lengthened to about 436 days for OMCT. Here, the sensitivity of the numerical system with respect to the excitations becomes obvious, as modified resonance conditions lead to significant effects on the free polar motion.

As pressure forcing is not regarded in ECCO, atmospheric pressure over the oceans has been eliminated in the applied NCEP data set. Hence, there is a conceptual difference between the ECHAM3 and NCEP forcing fields as atmospheric pressure over the oceans is contained in ECHAM3. Therefore, the annual polar motion due to ECHAM3 forcing is much stronger (152 mas) than in the case of NCEP (111 mas). The same holds for the oceanic induced polar motion, as the OMCT driven result is characterised by a strong annual signal (92 mas) which is very weak in the case of ECCO (29 mas). However, annual oscillations of the mass terms of ECHAM3 and OMCT are nearly out of phase, which indicates that the simulated oceanic response is very near to that of an inverted barometer. Consequently, annual atmospheric and oceanic contributions to polar motion compensate each other partially when the excitations are superposed.

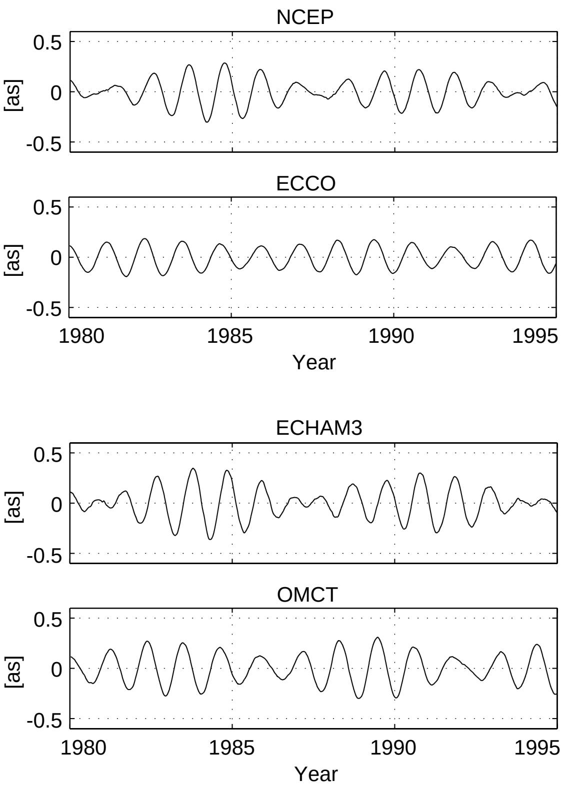

Figure 2. Model results for polar motion (x-component) applying separated atmospheric and oceanic excitations. Linear trends have been removed.

Thus, coupling between the two subsystems is essential when simulating their combined influence on polar motion.

Wavelet analyses of the time series reveal, that the Chandler oscillation is excited by both atmospheric and oceanic variations. The mean amplitudes of the Earth's free oscillation amount to 146 mas (NCEP), 132 mas (ECCO), 136 mas (ECHAM3), and 192 mas (OMCT). However, for both atmospheric model runs the Chandler amplitudes slightly decrease, whereas the amplitudes are rather stable (ECCO) or even slightly increase (OMCT) when DyMEG is driven by oceanic angular momenta.

4 Chandler wobble excitation

The results of the previous section show, that both atmospheric and oceanic forcing influences the free polar motion of DyMEG. In order to assess the excitation mechanism of the Chandler amplitude, the applied angular momentum series are analysed spectrally. In the following, solely the tensor elements $\Delta\underline{\mathbf{I}}_{13}$ and $\Delta\underline{\mathbf{I}}_{23}$ are regarded. The other deviation moments of the tensor influence polar motion only marginally (Munk and MacDonald, 1960). Though relative angular momenta have some influence on the amplitude of polar motion, they do not influence its general characteristics significantly (Seitz et al., 2004). Therefore, they shall be neglected, too.

The components $\Delta\underline{\mathbf{I}}_{13}$ and $\Delta\underline{\mathbf{I}}_{23}$ of the excitation series are considered as complex numbers with $\gamma(t) = \Delta\underline{\mathbf{I}}_{13}(t) - i\ \Delta\underline{\mathbf{I}}_{23}(t)$. Earlier, Brzezinski and Nastula (2000) and Gross (2000) concluded from spectral analyses of the complex excitation series of the NCEP reanalyses and an ocean model of the MIT, that the energy which is contained in a band between approximately 400 and 500 days is sufficient to excite the observed Chandler oscillation between 1985 and 1996. While the analyses of Gross revealed, that the largest part of the excitation energy can be ascribed to oceanic bottom pressure variations, Brzezinski and Nastula (2000) concluded, that the contribution of both subsystems is nearly equal. In contrast to these two studies, which were performed solely in the spectral domain, the resulting polar motion series are analysed here, too. First, it will be studied, if the signal energy contained in a symmetric band of ±30 days around the Chandler period (400-460 days) is sufficient, to maintain the Chandler

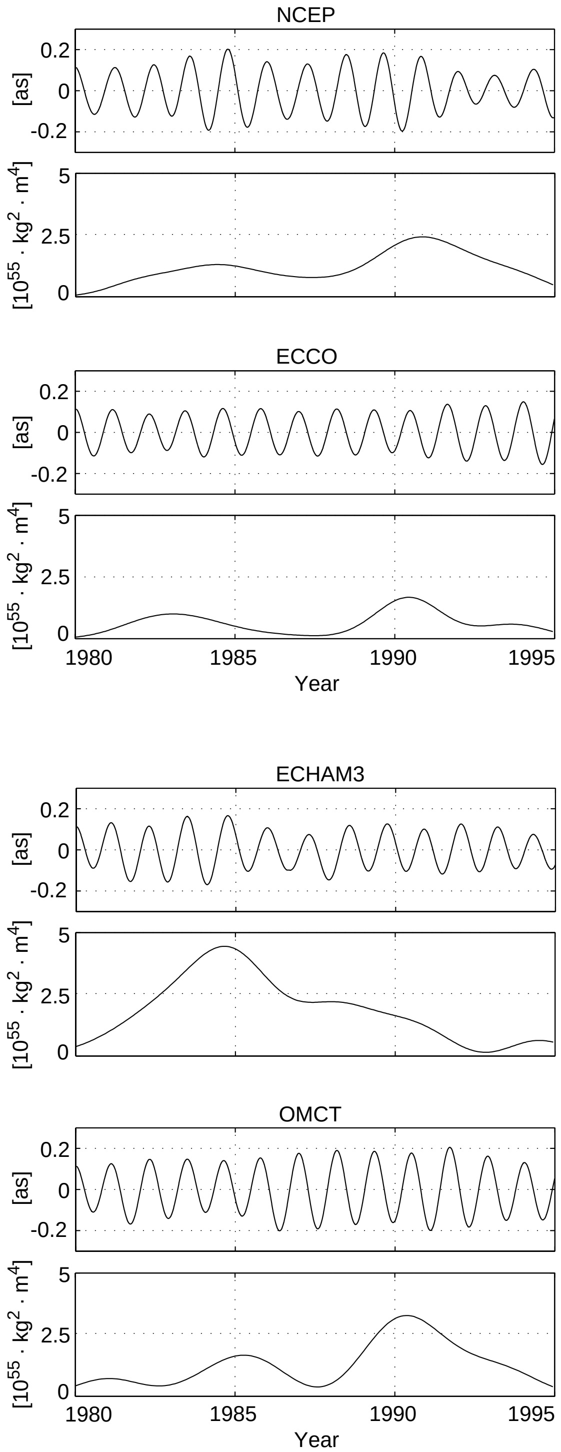

Figure 3. Model results for polar motion (x-component) applying band-pass filtered atmospheric and oceanic time series of the tensor elements $\Delta\underline{\mathbf{I}}_{13}$ and $\Delta\underline{\mathbf{I}}_{23}$ (upper panels) in comparison with the integral wavelet energy of the excitations in the spectral band between 400 and 460 days (lower panels).

amplitude of DyMEG by resonant interaction. This bandwidth was chosen in order to avoid spectral leakage from the annual into the Chandler band, which might adulterate the results. For this study, the complex excitation series are band-pass filtered, applying an elliptic Cauer-filter which is characterised by a very sharp pass-band. After multiple test runs, satisfactory agreement between the spectra of the filtered excitation series and the original tensor variations $\gamma(t)$ was achieved in the pass-band.

Fig. 3 shows the resulting polar motion (x-components) for the four band-pass filtered atmospheric and oceanic excitations (upper panels). In addition, the integral signal energy is displayed, which is contained in the prograde Chandler band of the respective complex time series $\gamma(t)$ between 400 and 460 days (lower panels). The signal energy has been determined by means of wavelet-transformation (Schmidt, 2001).

In all polar motion series, the Chandler amplitude does not increase or decrease continuously but features fluctuations which are linked to the instantaneous energy level of the excitation series $\gamma(t)$. The highest Chandler amplitudes are achieved for NCEP and OMCT while the ECCO run shows a rather weak amplitude. The mean amplitudes of the time series correspond to the values given in section 3.2. Both atmospheric data sets show a higher energy level than the corresponding ocean models. The energy of ECHAM3 is higher than the energy of NCEP, the level of OMCT is higher than the one of ECCO (cf. Thomas et al., 2005).

In the case of NCEP and ECHAM3, the maxima of the energy and the maxima of the Chandler amplitude are syncing. For OMCT and ECCO, the temporal agreement of energy and amplitude is not so conspicuous. Obviously not only the amount of excitation energy in the Chandler band but also the instantaneous phase relations of the excitations and the Chandler wobble are very important. Hence, the knowledge of the absolute amount of excitation energy does not allow for a definite conclusion of the resulting Chandler amplitude. Nevertheless, this experiment reveals, that the energy of the atmospheric and oceanic excitations is high enough to counteract the damping of the Chandler wobble.

In a second experiment, the excitations $\gamma(t)$ are substituted by equally distributed random numbers (white noise) from the interval $[-1, +1]$

(Units [kg m^2]). This purely synthetic excitation is multiplied by a constant factor l which corresponds to a variation of the noise level. Instead of $\Delta\underline{\mathbf{I}}_{13}$ and $\Delta\underline{\mathbf{I}}_{23}$, two of these time series are introduced into DyMEG. As expected, no reaction of the gyro becomes obvious for small values of l. For $l = 1 \cdot 10^{27}$, first effects on the free rotation of DyMEG are visible as the damping is attenuated. For $l = 1 \cdot 10^{29}$ the white noise is fully capable of exciting the Chandler wobble. The results of three model runs with different random excitations (all with $l = 1 \cdot 10^{29}$) are displayed in Fig. 4. Analogous to Fig. 3, the integral wavelet energy in the Chandler band (400-460 days) is shown, too.

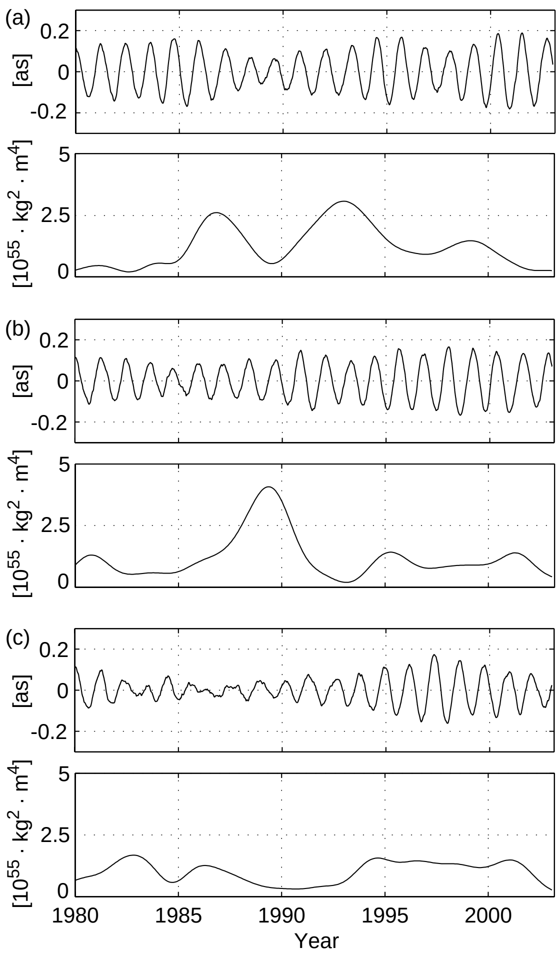

Figure 4. Model results for polar motion (x-component) applying three different time series of equally distributed random numbers from the interval $[-1 \cdot 10^{29}, +1 \cdot 10^{29}]$ kg m^2 instead of the tensor elements $\Delta\underline{\mathbf{I}}_{13}$ and $\Delta\underline{\mathbf{I}}_{23}$.

As clearly visible, the Chandler wobble is excited by the white noise. The noise level, which is necessary for the perpetuation of the Chandler amplitude corresponds to the noise level which is described by the atmospheric and oceanic excitations (cf. Fig. 3). As above, the maxima of the energy and the maxima of the Chandler amplitude are not always syncing. Hence, this result supports the assumption, that not the energy level alone, but also the instantaneous phases of the random excitations are very important for the excitation of the Chandler wobble.

Which atmospheric and oceanic processes are responsible for the noise, cannot be resolved in detail. It is assumed that purely stochastic atmospheric variations (weather) contribute essentially to the noise. As atmosphere and oceans interact, the stochastic signal is carried forward from the atmosphere into the oceans.

5 Conclusions

The numerical results of this study show, that noise which is contained in the time series of atmospheric and oceanic angular momentum variations, is sufficient to excite the Chandler wobble of the dynamic model DyMEG over more than two decades. The resonant reaction of the model on the stochastic forcing is caused by rotational deformations. Experiments with synthetic random excitations reveal, that the amount of energy which is necessary for the maintenance of the Chandler amplitude is just as high as the energy level of both atmospheric and oceanic excitations in a band between 400 and 460 days. As no deterministic signals were found in the Chandler band of the excitation series, it is assumed, that the existent energy is due to stochastic weather phenomena which yield a flat distribution of energy over the whole spectrum. Via atmosphere-ocean interaction, the noise is transferred into the oceans.

Acknowledgements

This paper was developed within a project supported by DFG grants DR 143/10 and HE 1916/4-1. The authors thank the Deutsches Klimarechenzentrum, Hamburg, Germany, for providing the ECHAM3 data set. NCEP reanalysis data was provided by the NOAA-CIRES Climate Diagnostics Center, Boulder CO, USA.

References

Brzezinski, A., and J. Nastula (2000). Oceanic excitation of the Chandler wobble, *Adv. Space Res.*, 30, No. 2, 195-200.

DKRZ (Deutsches Klimarechenzentrum) Modellbetreuungsgruppe (1992). *The ECHAM3 atmospheric general circulation model*, Techn. Rep. 6, Hamburg.

Gross, R. (2000). The excitation of the Chandler wobble, *Geophys. Res. Lett.*, 27, No. 15, pp. 2329-2332.

Kalnay, E., M. Kanamitsu, R. Kistler et al. (1996). The NCEP/NCAR 40-Year Reanalysis Project, *Bull. Amer. Meteor. Soc.*, 77, pp. 437-471.

Munk, W. and G. MacDonald (1960). *The Rotation of the Earth. A Geophysical Discussion.* Cambridge University Press, Cambridge.

Schmidt, M. (2001). Wavelet analysis of stochastic signals. In: *High frequency to subseasonal variations in Earth rotation.* Kolaczek, B., H. Schuh and D. Gambis (eds.), IERS Technical Note 28, Observatiore de Paris, pp. 65-72.

Seitz, F. and H. Kutterer (2002). Numerical Solutions for the non-linear Liouville equation. In: *Vistas for Geodesy in the New Millennium.* Adam, J. and K.P. Schwarz (eds.), IAG-Symposia 125, Springer, Berlin, pp. 463-468.

Seitz, F. and H. Kutterer (2005). Sensitivity Analysis of the non-linear Liouville equation. In: *A Window on the Future of Geodesy.* Sansó, F. (ed.), IAG-Symposia 128, Springer, Berlin, pp. 601-606.

Seitz, F., J. Stuck and M. Thomas (2004). Consistent atmospheric and oceanic excitation of the Earth's free polar motion, *Geophys. J. Int.*, 157, pp. 25-35.

Smith, M. and F. Dahlen (1981). The period and Q of the Chandler wobble, *Geophys. J. R. Astr. Soc.*, 64, pp. 223-281.

Stammer, D., C. Wunsch, R. Giering et al. (2003). Volume, heat and freshwater transports of the global ocean circulation 1993-2000, estimated from a general circulation model constrained by World Ocean Circulation Experiment (WOCE) data, *J. Geophys. Res.*, 108, 10.1029/2001JC001115.

Stuck, J., F. Seitz and M. Thomas (2005). Atmospheric forcing mechanisms of polar motion. In: *Forcing of polar motion in the Chandler frequency band: A contribution to understanding interannual climate variations.* Plag, H.-P., B. Chao, R. Gross and T. van Dam (eds.), Cahiers du Centre Européen de Géodynamique et de Séismologie 24, Luxembourg.

Thomas, M., J. Sündermann and E. Maier-Reimer (2001). Consideration of ocean tides in an OGCM and impacts on subseasonal to decadal polar motion excitation, *Geophys. Res. Lett.*, 28, No. 12, pp. 2457-2460.

Thomas, M., H. Dobslaw, J. Stuck and F. Seitz (2005). The ocean's contribution to polar motion excitation - as many solutions as numerical models?. In: *Forcing of polar motion in the Chandler frequency band: A contribution to understanding interannual climate variations.* Plag, H.-P., B. Chao, R. Gross and T. van Dam (eds.), Cahiers du Centre Européen de Géodynamique et de Séismologie 24, Luxembourg.